Northwest Africa 032, 479

Unbrecciated basalt

~300, 156 g

Figure 1: Cut face of a piece of NWA 479 ((photo courtesy of B. Fectay and C. Bidaut).

Introduction

Northwest Africa (NWA) 032 was found in the Saharan desert in October 1999, and weighs approximately 300 g. The stone is covered with fusion crust, but the exterior also has patches of white calcite and also red to orange ferric oxide or oxyhydroxide (Fagan et al., 2002; Korotev et al., 2001). The interior is an unaltered unbrecciated crystalline basalt with phenocrysts of olivine, pyroxene and chromite (Figs 2 and 3). A paired stone, NWA 479 (Fig. 1) weighing 156 g (Barrat et al., 2001, 2005), is the exact missing half as matched by the respective owners (B. Fectay, personal communication, 2007).

Petrography and Mineralogy

Olivine (11.3%), Pyroxene (4.8%), and chromite (0.3%) phenocrysts are in a groundmass (80.4%) of feldspar, pyroxene, ilmenite, troilite and metal. There are ubiquitous shock melt veins (3.2%). Olivine phenocrysts are zoned from Fo_{66} cores to Fo_{50} rims. Pyroxenes exhibit a large compositional range from low Ca bronzites to close to pyroxferrite at the FeO-rich end (Fig. 4). Pyroxenes from NWA 479 completely overlap

Figure 2: close up of cut slab of NWA 032 illustrating the olivine phenocrysts in a dark grey groundmass.

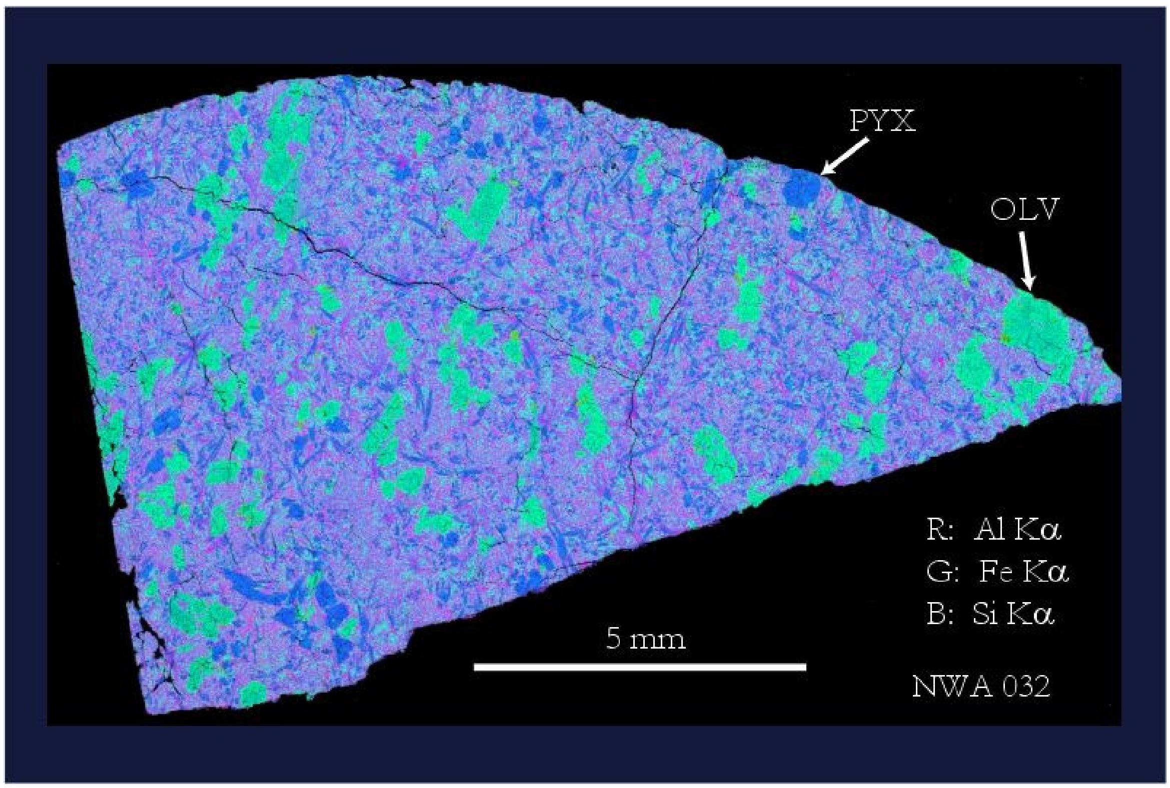

Figure 3: X-ray map of a thin section of NWA 032 showing green olivine phenocrysts, blue pyroxenes, and a purplish groundmass (from Fagan et al., 2003).

those found in NWA 032 (Fig. 5). Chromites are zoned from Cr-rich cores to ulvospinel rims (Fig. 6). Undulatory/mosaic extinction in the olivine and pyroxene, along with the presence of ringwoodite and wadsleyite in shock melt veins from NWA 479, attest to the high shock state of these meteorites.

Textures similar to that of NWA 032 have been experimentally reproduced by initial slow cooling to form olivine phenocrysts followed by more rapid cooling (5 °C/hr) to form the pyroxene-rich mesostasis (Koizumi et al., 2006). Such a sample could have formed near the top (close to the chilled margin) of a large basaltic magma body represented by the NWA and LAP lunar meteoritic basalts (Day and Taylor, 2007).

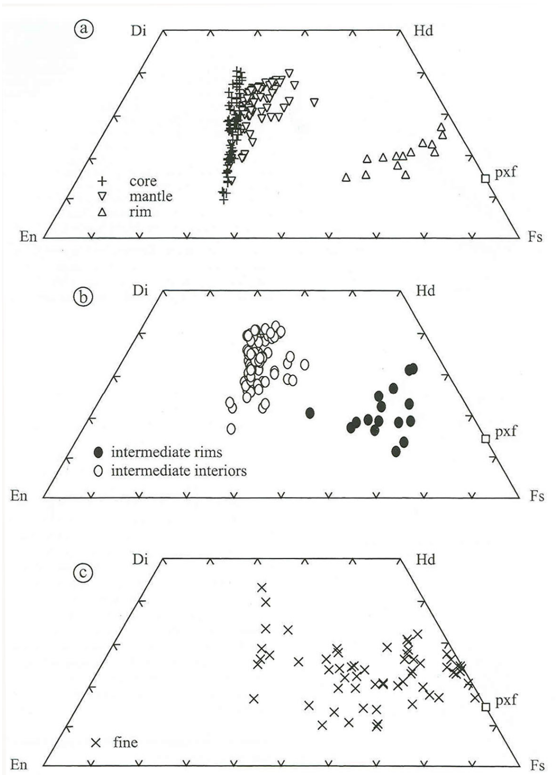

Figure 4: Pyroxene compositions from NWA 032 including phenocrysts (top), intermediate (middle) and fine grained (bottom) (from Fagan et al., 2002).

Figure 5: compositions from NWA 479 showing overlap with NWA 032 pyroxenes (from Barrat et al., 2005).

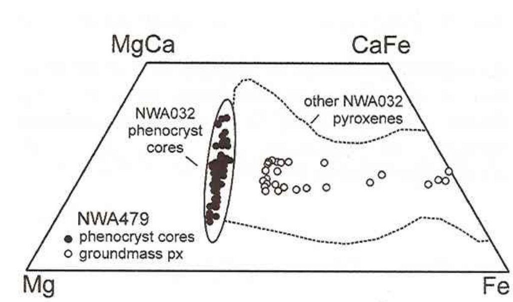

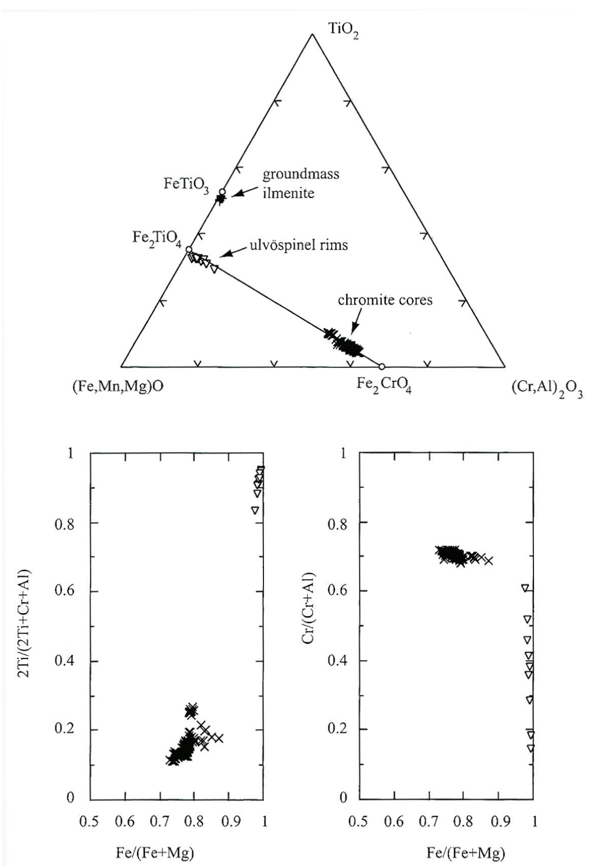

Figure 6: Spinel cores and rims from NWA 032 (Fagan et al., 2002).

Chemistry

NWA 032 has a composition very similar to low Ti basalt such as those found in the Apollo 12 and 15 collection (Fig. 7 and 8; Table 1). It represents a liquid composition because the olivine phenocryst cores are identical in composition to those expected from the bulk composition and Mg-Fe Kd (Fagan et al., 2002). Both NWA 032 and NWA 479 exhibit LREE enrichment (Fig. 9 and 10), have high Th/Sm. The latter cannot be due to magmatic fractionation from a more familiar parental liquid, since there is no known major phase that will fractionate these two elements. Instead it may be from a region of the Moon unsampled by Apollo or Luna collections. This has also been suggested based on the depleted Nd isotopic values, coupled with LREE/HREE and Th/HREE (Borg et al., 2007). Additionally, olivine phenocrysts record variable and heavy Li isotopic composition, having δ^7Li as high as +15, compared to much lower (0 to +4) for terrestrial mantle (Barrat et al., 2005). The variation has been ascribed to diffusivity control, but the heavy character of the values has been attributed to the giant impact that formed the Moon.

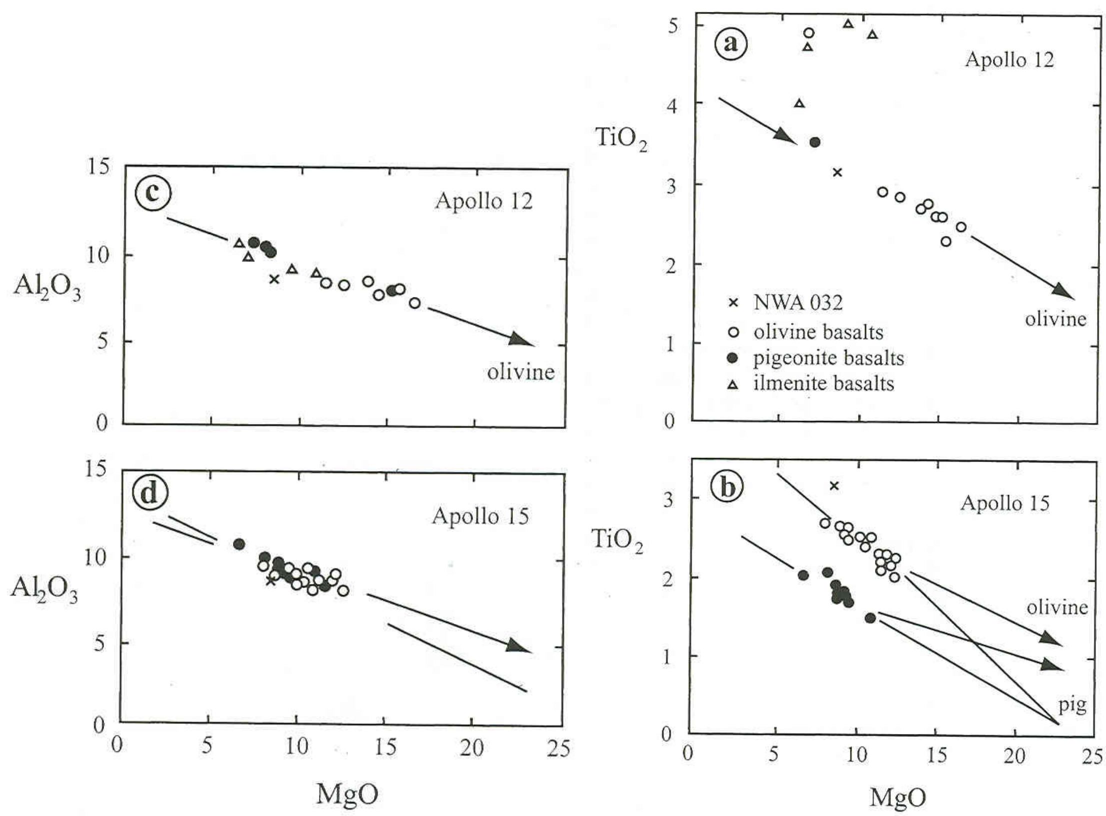

Figure 7: Al_2O_3 vs. MgO for NWA 032 (x) compared to Apollo 12 and 15 basalts.
Figure 8: TiO_2 vs. MgO for NWA 032 (x) compared to Apollo 12 and 15 basalts, showing fractionation vector for olivine and pigeonite (from Fagan et al., 2002).

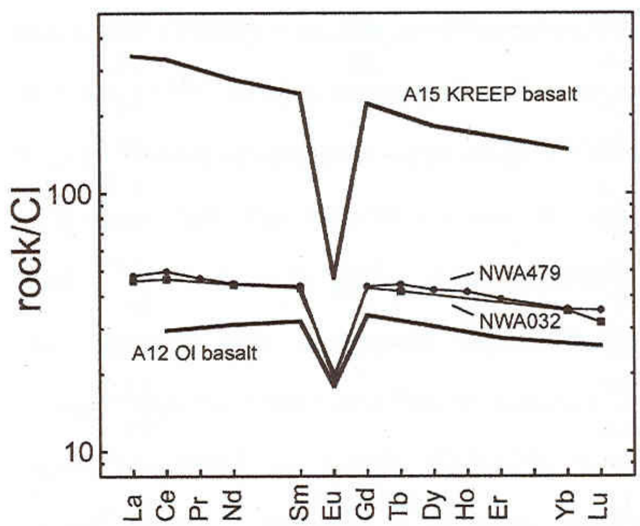

Figure 9: Rare earth element patterns for NWA 032 and 479, compared to Apollo 12 olivine basalt and KREEP illustrating their LREE nature (from Barrat et al., 2005).

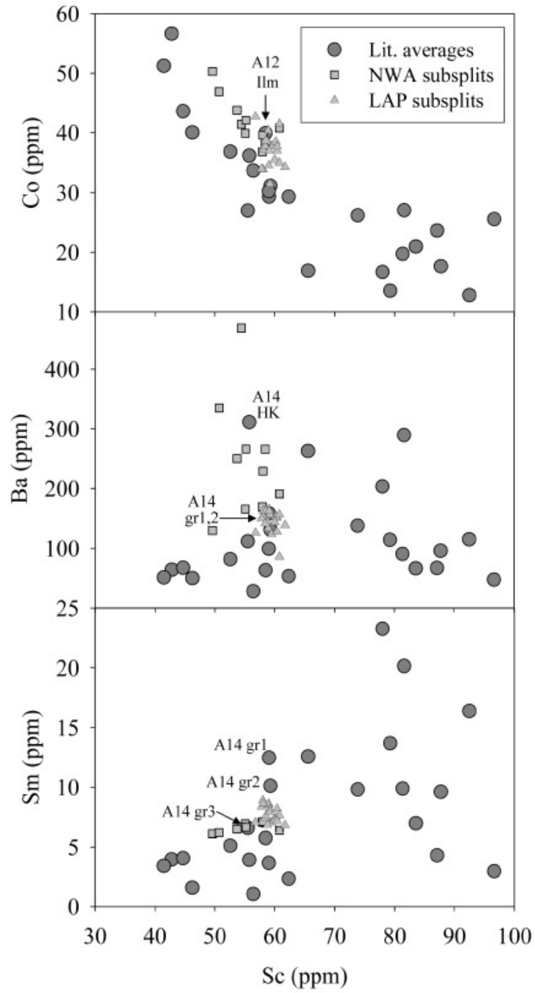

Figure 10: Co, Ba and Sm vs. Sc (all in ppm) for the NWA 032 subsamples analyzed by Zeigkler et al. (2005), compared to average mare basalt compositions from the Apollo and Luna missions (dark grey circles).

Radiogenic age dating

^{39}Ar-^{40}Ar plateau ages for splits of NWA 032 and NWA 479 yield similar ages of 2775 and 2734 Ma, respectively (Fig. 11; Fernandes and Burgess, 2006b; Fagan et al., 2002; Fernandes et al., 2003). Also, Rb-Sr and Sm-Nd ages of 2852 (±65) and 2692 (±160) Ma have been measured in NWA 032, within error of the Ar-Ar ages (Borg et al., 2007).

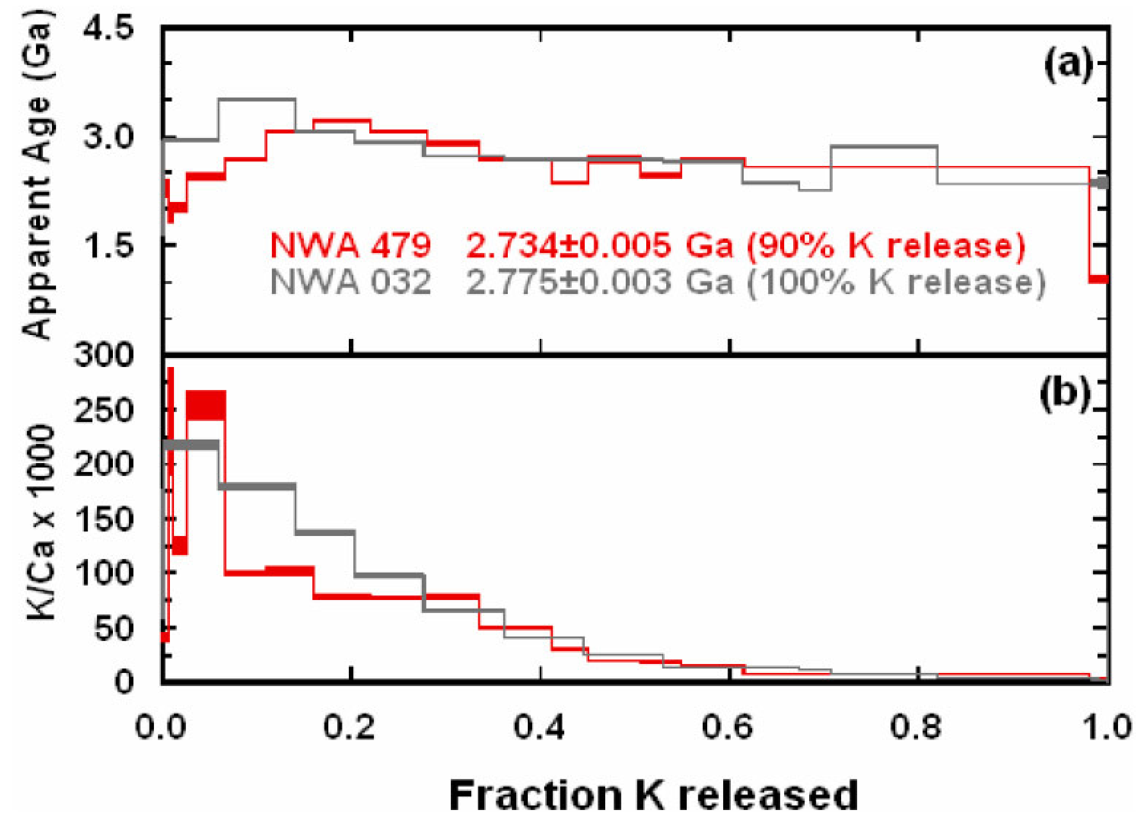

Figure 11: Comparison of apparent age and Ca/K for NWA 032 and NWA 479 (from Fernandes and Burgess, 2006b).

Cosmogenic isotopes and exposure ages

Residence time in the lunar regolith has been measured by Fernandes et al. (2003) and Lorenzetti et al. (2005) at 212 Ma and 207 Ma, respectively. The large fluence of 2.58 x 10^{16} n cm^{-2} is also consistent with the large CRE (Hidaka and Yoneda, 2006). However, Lorenzetti et al. (2005) argue that NWA 032 experienced a multi-stage exposure at different shielding depths. The transit time from Moon to Earth was 0.042 Ma, terrestrial residence time < 0.01 Ma, and a therefore a time of ejection of 0.05 Ma (Lorenzetti et al., 2005).

Table 1. Chemical composition of NWA 032/479

reference	1	2	3	4	4	4	4	4	4	4	4	4	4	4
				9	21	8.1	10.7	9.6	7.7	18.2	15.6			Std
Weight (mg)	550	184	132									24.2	124	dev
method	g	e	a,b											
SiO_2 %	44.7			45.1	44.2	45.4	45.6	43.4	44.5	44.7	44.5	45.2	44.7	0.015
TiO_2	3.08		3.15	2.85	2.96	3.01	3.33	2.63	3.08	3.02	2.82	3.15	3	0.068

Al_2O_3	8.74		9.48	9.42	9.02	9.42	9.9	8.67	9.99	9.37	8.58	9.73	9.32	0.054
FeO	23	22.1	20.94	0.4	0.37	0.37	0.36	0.42	0.39	0.56	0.36	0.38	0.4	0.154
MnO	0.33		0.29	21.7	22.6	22.1	21.5	23.7	21.8	22.6	22	21.8	22.2	0.031
MgO	8.45		7.21	0.27	0.28	0.29	0.27	0.3	0.26	0.26	0.29	0.3	0.28	0.06
CaO	10.9		10.99	7.97	8.5	7.36	6.3	10.26	6.86	7.64	9.85	6.92	7.97	0.17
Na_2O	0.37	0.347	0.34	10.7	10.4	10.9	11.5	9.5	11.3	10.4	9.8	10.9	10.6	0.062
K_2O	0.11		<0.1	0.36	0.34	0.35	0.38	0.33	0.37	0.32	0.34	0.35	0.35	0.052
P_2O_5				0.08	0.09	0.09	0.11	0.08	0.1	0.1	0.11	0.09	0.09	0.122
S %														
sum				99	98.9	99.3	99.3	99.3	98.8	99.1	98.8	98.9	99.0	0.088
Sc ppm		56	61	60.8	53.7	58	57.9	49.6	55.1	50.7	54.4	58.4	55.2	0.067
V			132											
Cr		2744	2614	2760	2500	2500	2430	2870	2660	3800	2490	2600	2760	0.154
Co		42	40.6	40.8	43.8	39.6	36.8	50.3	39.9	46.9	41.4	38.5	42.1	0.102
Ni		50	49.2											
Cu			34.2											
Zn			30.5											
Ga			4.31											
Ge														
As														
Se														
Rb			1.78											
Sr		142	132	126	140	130	160	140	126	190	160	140	149	0.14
Y			65.71											
Zr		175	206	160	170	180	180	160	160	160	170	180	170	0.055
Nb			15.26											
Mo														
Ru														
Rh														
Pd ppb														
Ag ppb														
Cd ppb														
In ppb														
Sn ppb														
Sb ppb														
Te ppb														
Cs ppm			0.051											
Ba		242	371	191	250	229	170	130	166	335	469	266	266	0.392
La		11.2	11.75	10.5	11.1	11.9	12.1	10.3	11.7	10.5	11.7	11.9	11.3	0.062
Ce		29.7	31.77	28.5	28.9	32.3	32.3	28.2	31.6	27.7	30.9	30.5	29.9	0.06
Pr			4.52											
Nd		21	21.21	19	18	22	22	16	20	19	21	21	20	0.098
Sm		6.61	6.73	6.37	6.48	7.1	7.05	6.1	6.92	6.18	6.64	6.98	6.63	0.058
Eu		1.1	1.13	1.06	1.07	1.15	1.2	1	1.15	1.02	1.13	1.17	1.1	0.064
Gd			8.9											
Tb		1.56	1.66	1.52	1.52	1.65	1.67	1.44	1.6	1.46	1.59	1.65	1.57	0.054
Dy			10.73											
Ho			2.35											
Er			6.46											

Tm													
Yb	5.79	5.86	5.7	5.7	6.1	6.2	5.3	6	5.4	5.8	6.1	5.8	0.053
Lu	0.802	0.893	0.81	0.78	0.85	0.85	0.74	0.83	0.75	0.81	0.83	0.8	0.052
Hf	5	5.05	4.76	4.96	5.29	5.31	4.55	5.13	4.63	5.1	5.32	5.02	0.059
Ta	0.62	0.8	0.56	0.64	0.71	0.68	0.6	0.61	0.6	0.61	0.65	0.63	0.073
W ppb		310											
Re ppb													
Os ppb													
Ir ppb													
Pt ppb													
Au ppb	4												
Th ppm	1.9	2.01	1.74	1.91	1.99	2.04	1.67	1.96	1.72	1.87	2.03	1.89	0.074
U ppm	0.45	0.46	0.35	0.44	0.44	0.45	0.39	0.4	0.51	0.57	0.49	0.46	0.144
Li ppm		12.69											
Be		1.22											
C													
S													
F ppm													
Cl													
Br													
I													
Pb ppm		1.02											
Hg ppb													
Tl													
Bi													

technique (a) ICP-AES, (b) ICP-MS, (c) IDMS, (d) EMPA, (e) INAA, (f) XRF, (g) wet chemistry

References: 1) Fagan et al. (2002); 2) Korotev et al. (2001); 3) Barrat et al. (2005); 4) Zeigler et al. (2005)